

Three-dimensional printed millimetre wave dielectric resonator reflectarray

ISSN 1751-8725
Received on 31st March 2017
Revised 21st July 2017
Accepted on 5th September 2017
E-First on 24th October 2017
doi: 10.1049/iet-map.2017.0278
www.ietdl.org

Shiyu Zhang¹ ✉

¹Wolfson School of Mechanical, Electrical and Manufacturing Engineering, Loughborough University, Leicestershire LE11 3TU, UK

✉ E-mail: s.zhang@lboro.ac.uk

Abstract: Reflectarray antennas have attracted extensive attention due to their low loss, high gain, compact volume, and their excellent abilities to control the radiated beam. The use of dielectric resonators as the reflectarray elements minimises the ohmic loss and the coupling between elements. This study uses fused deposition modelling (FDM) three-dimensional (3D) printing rapidly prototyping a low cost and light-weight dielectric resonator reflectarray. The demonstrated reflectarray is composed of 625 3D printed dielectric resonator elements to control the reflected phase over the reflector surface. The total size is $12 \times 12 \text{ cm}^2$ and the mass is 67 g. Measurements show that this reflectarray provides 28 dBi gain at 30 GHz when offset fed by a Ka-band horn antenna. This work demonstrates the potential of FDM for millimetre wave (mm-wave) applications. The new 3D printing approach can be deployed for high-gain mm-wave antenna fabrication with significantly reduced labour time and material costs.

1 Introduction

Reflectarrays are able to reflect the waves that are transmitted from a feed source into a planar phase wavefront at a desired angle and vice versa. They can be used to produce high-gain antennas with a pencil beam in the specific direction. Reflectarrays do not have the complex and lossy feed network when compared with phased arrays and have numerous advantages, including their low cost, small size and weight, and low profile when compared with traditional parabolic reflectors [1, 2]. The flat profile reduces the required volume which is of particular interest to spacecraft and satellites.

The array elements on a reflectarray yield a variable phase distribution, which compensates the path length differences from the feed source to the elements. Therefore, the entire reflectarray can produce a collimated beam in a desired direction. Most conventional reflectarrays are based on metallic resonators, typically microstrip elements that are printed on substrates. They suffer from ohmic and surface wave loss, and narrow bandwidth [3–5]. A viable alternative to metallic elements is using dielectric array elements. Generally, there are two ways to realise the dielectric array elements depending on the material availability and the fabrication technique: (i) use one dielectric slab with locally varied effective permittivity for the phase control; and (ii) use dielectric resonators with various dimensions for tuning the local reflected phase. The former approach has been reported in [6, 7], and the reflectarrays are similar to the perforated or grooved Fresnel zone plate reflectors. The second approach uses discrete resonators as array elements and it gives extra freedom in modifying the individual elements. The individual element is similar to dielectric resonator antennas (DRA) that provides the benefits of lower loss, relatively wider bandwidth, higher efficiency, and smaller mutual coupling between elements [8, 9]. Therefore, the dielectric resonator reflectarrays have the potentials of offering wider bandwidth and higher gain [10]. However, the manufacturing processes for the dielectric resonator reflectarrays are generally cumbersome and do not make this approach attractive. Multi-step and high-tolerance fabrication processes such as spin-coating, electron beam lithography, and milling are involved to ensure the subwavelength sized dielectric resonator elements are secured at specific locations with correct dimensions [11–13].

Three-dimensional (3D) printing is an additive manufacturing (AM) technique that allows the creation of arbitrary 3D geometries without machining, and therefore it simplifies the fabrication process and reduces the cost. With the advent of AM, the dielectric components can be rapidly and inexpensively prototyped in-house. There are a number of studies that have shown 3D printed millimetre wave antenna components that used for realising circular polarisation and enhancing antenna gain [14, 15]. Dielectric materials with locally tailored dielectric constant could also be directly 3D printed and applied for graded index lenses and Fresnel lenses applications [16, 17]. Nayeri *et al.* [7] have demonstrated using 3D printing to fabricate the reflectarrays, but the array elements were not resonator structures. On the other hand, the PolyJet 3D printers that used in [7] are generally expensive and the material options for the PolyJet are limited by the manufacturer. The relative permittivities of the polymers that are used for PolyJet are mostly >3 . This is a challenge for fabricating dielectric resonators as they usually require high permittivity materials. The discrete dielectric resonator array element can be realised if a high permittivity material is used and the gain and aperture efficiency of the reflectarrays can be improved. However, there is no report for the 3D printed dielectric resonator reflectarray yet.

In this paper, the low-cost fused deposition modelling (FDM) is used for fabricating a dielectric resonator reflectarray. FDM is one of the 3D printing techniques and it uses the low-cost thermoplastic [e.g. polylactic acid and acrylonitrile butadiene styrene (ABS)] based materials. The raw materials can be mixed with additives to increase the relative permittivity or mechanical strength. This gives extra freedom to customise the 3D printing materials [18]. Composite structures with the desired set of properties over a wide range of frequencies can therefore be constructed. The composite ABS material has been used in this work, and a light-weight dielectric resonator reflectarray that produces a high-gain collimated beam in the boresight direction from an offset feed has been 3D printed. To the author's best knowledge, this is the first to report the use of FDM to fabricate periodical array structures up to Ka-band. This new approach minimises the material usage and processing time for high-gain antenna applications.

This paper is organised as follows. Section 2 introduces the dielectric resonator array element design and its phase tenability. Section 3 presents the phase distribution on the reflectarray and the details of 3D printing fabrication. The measurement results are

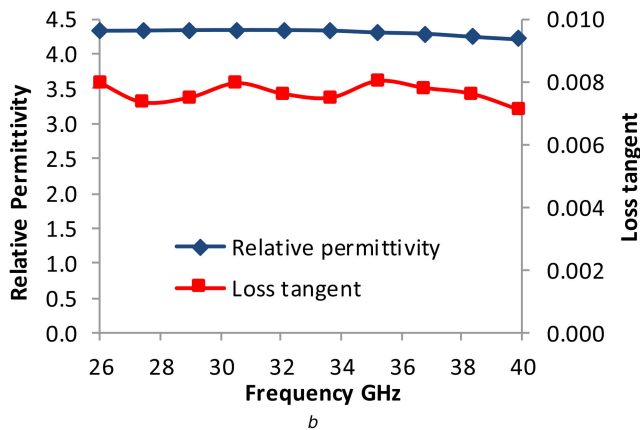
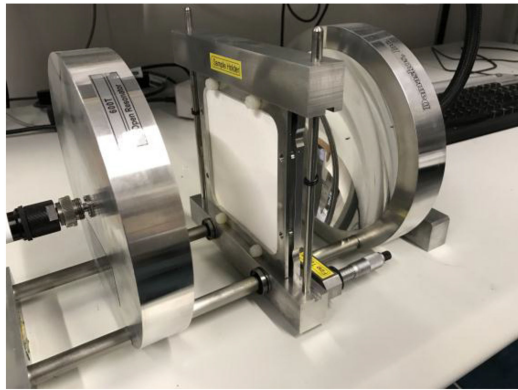


Fig. 1 Measurement of composite ABS material (a) Dielectric constant measurement set-up using the open resonator (b) Measured results of relative permittivity and loss tangent of the composite ABS sample at Ka-band

shown in Section 4 and compared with the full-wave simulations. Section 5 concludes the paper.

2 Array element configuration and phase changes

Sourcing a suitable AM material is the first challenge that needs to be addressed for successfully 3D printing the DRAs as the reflectarray elements. The relative permittivity (ϵ_r) is typically ~ 2.7 for most AM polymer materials which makes them not ideally suited for DRA applications. Increasing the ϵ_r of the AM materials can realise more compact DRA designs and hence makes them more suitable for array elements in a reflectarray.

The AM material used in this work was a composite ABS-based material (PREPERM® TP20280). Submicron scale dielectric particles were added into the ABS and increased the ϵ_r from 2.7 to 4.4. This makes it a candidate for dielectric resonators that provide the essential phase shift in the reflectarray. After mixing, the mixture was melted and extruded into the filament form that can be used for general FDM 3D printing. A dielectric slab was printed and measured by using the open resonator (from Damaskos [19]) at Ka-band frequency. The measurement set-up and the measured dielectric constant and loss tangent as a function of frequency are shown in Fig. 1. This ABS filament can be smoothly extruded with the temperature from 210 to 230°C.

The reflected phase response of a dielectric resonator unit cell with such dielectric properties was analysed by using CST Microwave Studio. The unit cell of the array element is shown in Fig. 2a. The reflectarray was designed to work at the centre frequency of 30 GHz, and the periodicity p was $\lambda_0/2 = 5$ mm that had been chosen in order to reduce the grating lobes. The unit cell was composed of a cuboid dielectric resonator element and a thin base layer. The base allowed the unit cells to maintain a constant periodicity, p , and allowed the whole reflectarray to be placed on a surface. The thickness of the base t (0.2 mm) was chosen to

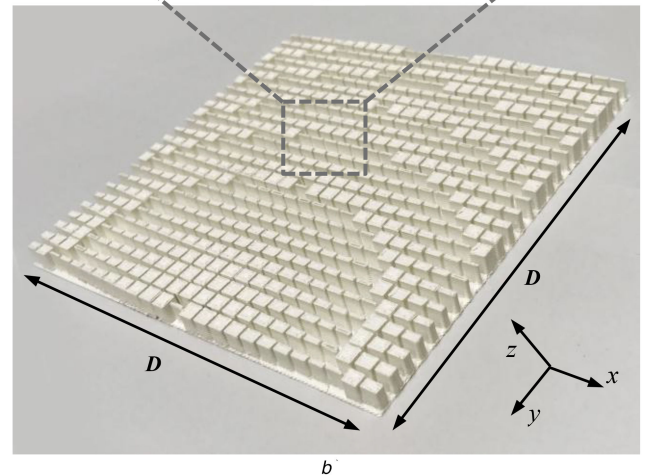
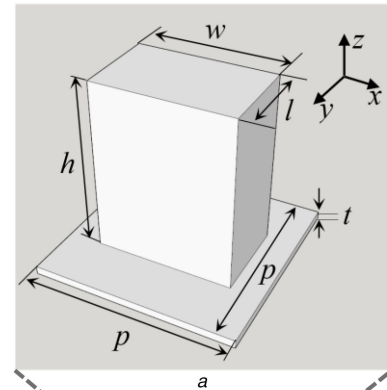


Fig. 2 Geometry of the 3D printed dielectric resonator reflectarray (a) Sketch of the unit cell of array elements (b) Photo of the 3D printed dielectric resonator reflectarray

Table 1 Design parameters of the unit cell of the dielectric resonator reflectarray

Name	Description	Value in mm
w	width of resonator	4.2
t	thickness of base	0.2
h	height of resonator	6.3
p	periodicity of unit cells	5.0
l	length of resonator	0.5–4.5
D	length of entire reflectarray	120

minimise the effect of the base but also allowed the reflectarray to be removed from the printer platform without damage. The design parameters of the unit cell are shown in Table 1. The length, l , was the variable that altered the reflection phase of the dielectric resonator at different oblique incident angles. The length of the individual dielectric resonator elements was varied from 0.5 to 4.5 mm in 0.1 mm steps. Fig. 2b shows the photo of the fabricated reflectarray.

Fig. 3 shows a 360° range of simulated phase change results was obtained by using the composite ABS material with $\epsilon_r = 4.4$ and $\tan\theta = 0.008$. The incident wave angle that produces the results in Fig. 3 was offset in the yz plane by 26.6° in the z -axis. The phase change of the conventional ABS ($\epsilon_r = 2.75$) was simulated for comparison. However, the unit cells with $\epsilon_r = 2.75$ were not able to provide a full range of 360° phase change with the same variation in dielectric resonator lengths, see Fig. 3.

3 Phase distribution and array fabrication

The phase distribution on the reflectarray aperture was designed based on the phase position of the feed and reflected beam angle. Here, the Cartesian coordinate was used to describe the location of the reflectarray and the feed. The reflectarray was placed in the xy plane, and the centre of the reflectarray was defined by $(x, y, z) =$

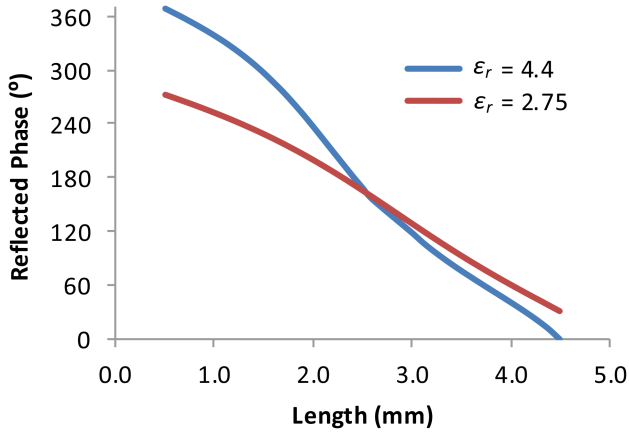


Fig. 3 Simulated phase response for parametric sweep of DRA length, at an operating frequency of 30 GHz

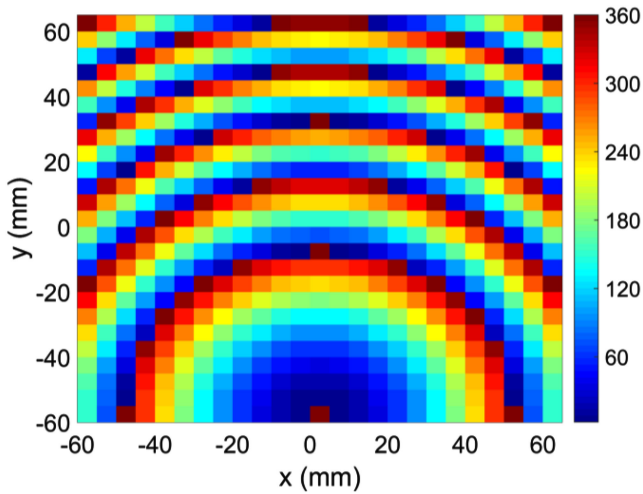


Fig. 4 Required phase distribution of the square reflectarray

(0, 0, 0). It was designed to produce a boresight reflected beam (θ_b , φ_b) along the z -axis; thus, it has $\theta_b = 0$ and $\varphi_b = 0$. In order to reduce the aperture blockage, an offset feed was chosen, and the feed point was defined by $(x_f, y_f, z_f) = (0, -60, 120)$ (in mm). The maximum incident angle should not exceed 45° to avoid the phase error at the edge of the reflectarray [1]. In this work, $F/D = 1$ was chosen. The feed was pointed at the centre (0, 0, 0) of the reflectarray. This resulted in the feed had a tilt angle of $\sim 26.6^\circ$ to point at the centre of the reflectarray. With this system set-up, the edge taper levels at the upper edge centre (0, 60, 0), lower edge centre (0, -60, 0), and two side edge centres ($\pm 60, 0, 0$) are -5.4 , -11.5 , and -11.5 dB, respectively. Now the required phase shift for the element i that is located at (x_i, y_i) can be determined by from (1) and (2):

$$\phi(x_i, y_i) = k_0[d_i - \sin \theta_b(x_f \cos \varphi_b + y_f \sin \varphi_b)] \quad (1)$$

$$d_i = \sqrt{(x_f - x_i)^2 + (y_f - y_i)^2 + (z_f - z_i)^2} \quad (2)$$

where k_0 is the propagation constant, and d_i is the distance from the feed point to the element i . The contour plot of the required phase distribution of the reflectarray is shown in Fig. 4.

Then the individual element dimensions could be determined according to: (i) the required phase shift at its location (Fig. 4); and (ii) the required length l to produce that phase shift from Fig. 3. The complete 3D model of the reflectarray was generated by using a MATLAB script and then imported into CST for full-wave analysis. The 3D model (STL format) was sent to the FDM printer for fabrication. Makerbot® Replicator™ 2X was used to 3D print the entire reflectarray in one-step process. The accuracy of the dimensions and the surface roughness of the printed objects were

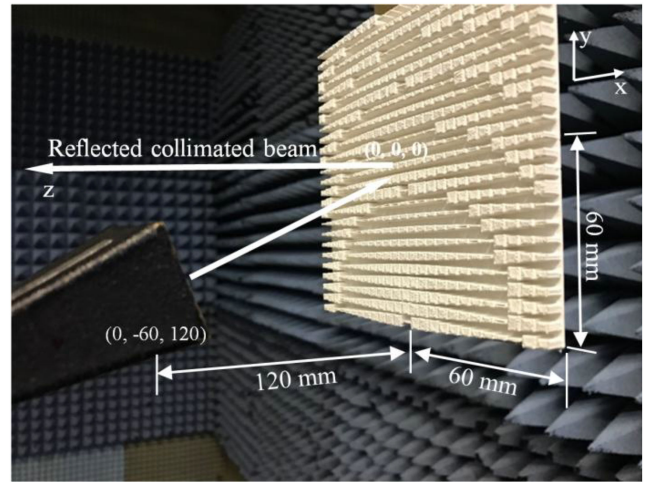


Fig. 5 Photo of the measurement set-up with reflectarray and offset feed

determined by the diameter of the printer nozzle and the resolution in z -axis that were chosen in the printer setting. The combination of fine nozzle and thin z -axis layer thickness would result in higher resolution and smooth surface but at the cost of longer print time. In this work, a fast print setting was used for rapidly prototyping. The printer nozzle that was used for printing was 0.4 mm diameter and the layer thickness in z -axis was 0.3 mm per layer. The final reflectarray was $120 \times 120 \text{ mm}^2$ with a total of 625 elements. The size of the reflectarray was limited by the print platform of this 3D printer. However, numerous low-cost FDM 3D printers with larger print platforms are commercially available. The total print time was ~ 3 h and the reflectarray (exclusive of ground plane) had a mass of ~ 67 g.

4 Simulation and measurement results

The 3D printed reflectarray was affixed on a $120 \times 120 \text{ mm}^2$ ground plane. A Ka-band horn antenna was used to illuminate the reflectarray with a distance of 120 mm between its phase centre (at 30 GHz) and the reflectarray plane (Fig. 5). The feed horn had gain of 18–20 dBi across the frequency range from 26 to 34 GHz and it had 19 dBi at 30 GHz with 19.9° and 20.5° half power beam widths (HPBW) in H-plane and E-plane, respectively. The electric field of the feed horn was simulated as a field source, and then the field source was used in the full-wave simulation to replace the feed horn structure for reducing simulation time.

The measured boresight gain of the 3D printed dielectric resonator reflectarray over the frequency range from 26 to 34 GHz is shown in Fig. 6, compared with the simulated gain results from CST. A good agreement between measurement and simulation was observed. The 3D printed dielectric resonator reflectarray had a maximum gain of 28 dBi at 30 GHz which was a 9 dB increase compared with the gain of the feed horn. Simulations indicated that the gain could be increased to 34 dBi if the size of the reflectarray was increased from $12\lambda^2$ to $24\lambda^2$. The -1 dB bandwidth of this reflectarray was $\sim 10\%$.

The radiation patterns of the reflectarray that were scanned from -90° to $+90^\circ$ in the H-plane (xz plane) and the E-plane (yz plane) at 30 GHz are shown in Figs. 7 and 8, respectively, and compared with results from the full-wave simulations. As it is shown in Figs. 7 and 8, boresight reflected pencil beams are observed, and measured radiation patterns agreed well with the simulated patterns. The agreement indicates that the fast print setting was good enough for fabricating the Ka-band dielectric resonator reflectarray. Owing to the offset feeding, the radiation pattern was asymmetrical in E-plane and the side lobe levels (SLL) in E-plane were greater than in H-plane. The SLL was -17.5 dB in H-plane and -25.5 dB in E-plane. The HPBW was $\sim 7^\circ$ for both E-plane and H-plane.

The offset fed resulted in the main beam scanning with frequencies. This was due to the change in phase taper across the reflectarray with a change in frequency. Since the feed horn was

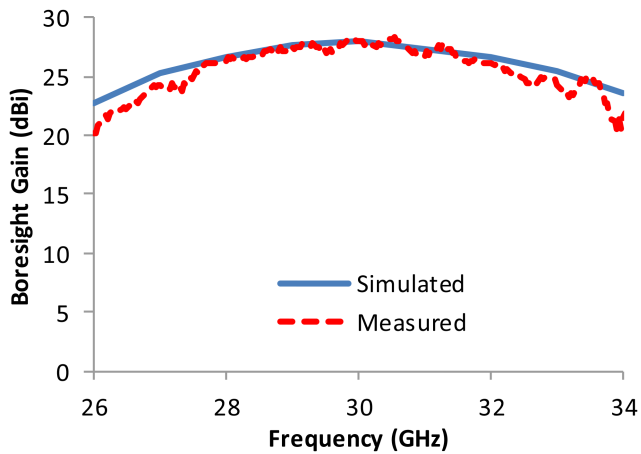


Fig. 6 Measured and simulated gain of 3D printed reflectarray fed by horn at an offset angle

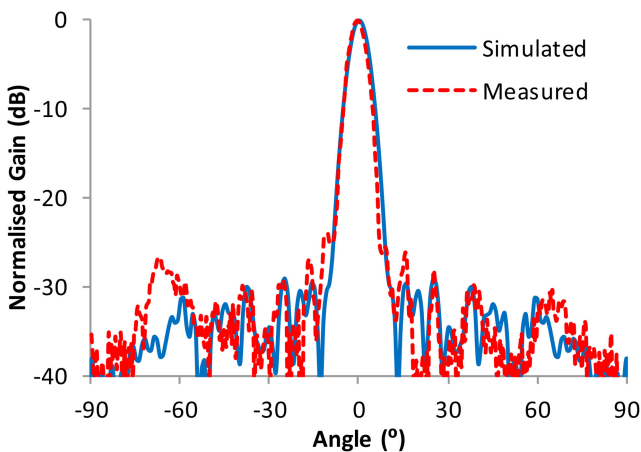


Fig. 7 Measured and simulated gain pattern at 30 GHz in the H-plane

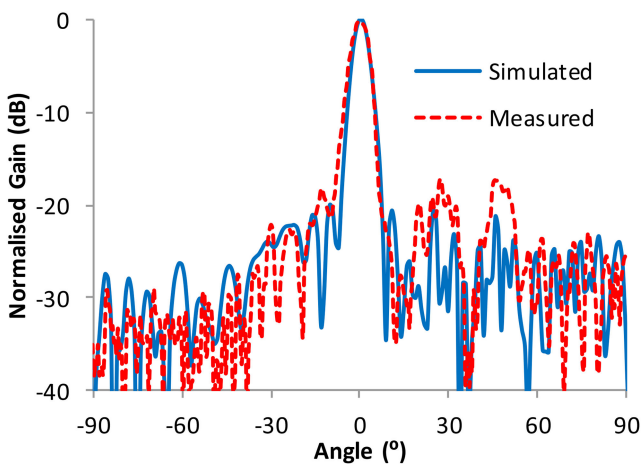


Fig. 8 Measured and simulated gain pattern at 30 GHz in the E-plane

only moved off-axis in E-plane, the beam squint was only observed in E-plane. The measured radiation patterns of the reflectarray in the H-plane and the E-plane are shown in Figs. 9 and 10, respectively (scanned from -45° to $+45^\circ$). Fig. 9 shows that the main beam are all reflected at 0° in the H-plane regardless of the frequency. Fig. 10 indicates that the maximum beam directions in E-plane are -3.6° (at 26 GHz), -0.9° (at 32 GHz), 0° (at 30 GHz), $+1.8^\circ$ (at 32 GHz), and $+2.3^\circ$ (at 34 GHz), respectively. The beam squint resulted in a reduced boresight gain, and therefore, it slightly reduced the bandwidth of the reflectarray. The beam squint could be minimised if the reflected angle was chosen to be close to the natural specular reflection angle [2]. The measured cross-polarisation patterns are shown in Figs. 9 and 10 and indicate the cross-polarisation level is well below -30 dB.

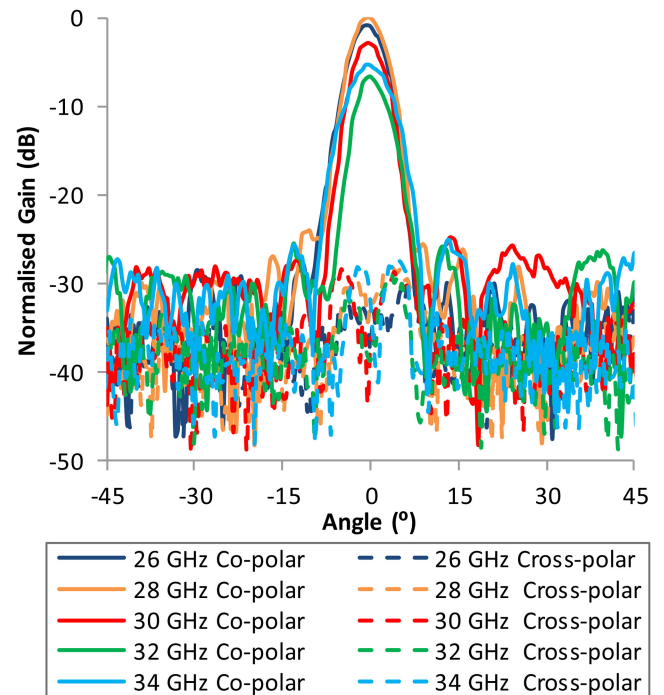


Fig. 9 Measured gain patterns over the frequency from 26 to 34 GHz in the H-plane

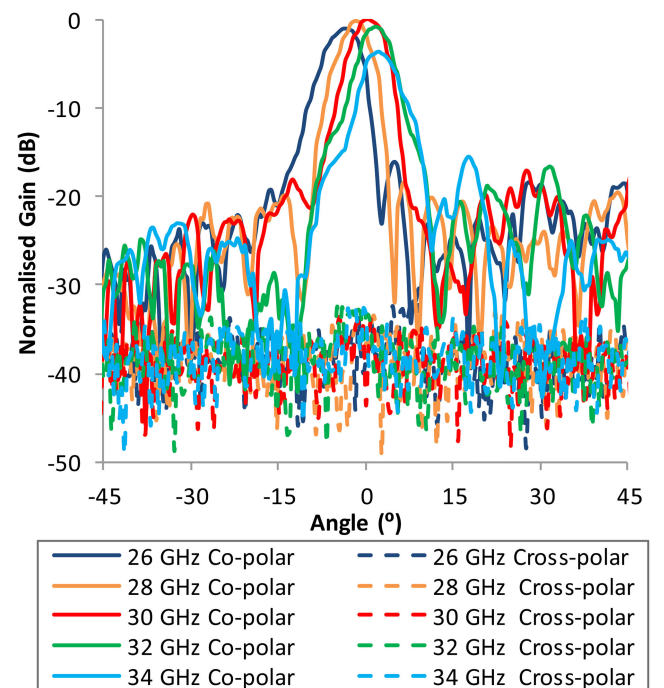


Fig. 10 Measured gain patterns over the frequency from 26 to 34 GHz in the E-plane

5 Conclusions

A dielectric resonator reflectarray has been successfully rapidly prototyped in a single-step process without any machining, by using the FDM 3D printing. This not only significantly reduced material waste but also simplified the manufacturing process and reduced the cost. The reflectarray was composed of 625 dielectric resonator elements with variable dimensions to produce the phase adjustments that yield a boresight collimated beam from an offset feed source. High-gain reflectarray and a pencil beam have been achieved. Measurements have demonstrated that this 3D printed reflectarray offered 20–28 dBi gain over the frequency range from 26 to 34 GHz when illuminated by a Ka-band rectangular horn antenna.

6 Acknowledgments

The author's work was supported by EPSRC Doctoral Prize Research Fellowship. The author thanks his colleagues Dr Will Whittow and Prof. Yiannis Vardaxoglou for valuable discussion concerning this work and thanks Premix for providing the 3D printing ABS filaments.

7 References

- [1] Huang, J., Encinar, J.A.: 'Reflectarray antennas' (John Wiley & Sons, Inc., 2008)
- [2] Pozar, D.M., Targonski, S.D., Syrigos, H.D.: 'Design of millimeter wave microstrip reflectarrays', *IEEE Trans. Antennas Propag.*, 1997, **45**, (2), pp. 287–296
- [3] Huang, J.: 'Bandwidth study of microstrip reflectarray and a novel phased reflectarray concept'. IEEE Antennas and Propagation Society Int. Symp. 1995 Digest, 1995, vol. 1, pp. 582–585
- [4] Encinar, J.A., Zornoza, J.A.: 'Broadband design of three-layer printed reflectarrays', *IEEE Trans. Antennas Propag.*, 2003, **51**, (7), pp. 1662–1664
- [5] Chen, H.-T., Taylor, A.J., Yu, N.: 'A review of metasurfaces: physics and applications', *Rep. Prog. Phys.*, 2016, **79**, (7), p. 76401
- [6] Abd-Elhady, M., Hong, W., Zhang, Y.: 'A Ka-band reflectarray implemented with a single-layer perforated dielectric substrate', *IEEE Antennas Wirel. Propag. Lett.*, 2012, **11**, pp. 600–603
- [7] Nayeri, P., Liang, M., Sabory-Garcia, R.A., *et al.*: '3D printed dielectric reflectarrays: low-cost high-gain antennas at sub-millimeter waves', *IEEE Trans. Antennas Propag.*, 2014, **62**, (4), pp. 2000–2008
- [8] Petosa, A., Ittipiboon, A.: 'Dielectric resonator antennas: a historical review and the current state of the Art', *IEEE Antennas Propag. Mag.*, 2010, **52**, (5), pp. 91–116
- [9] Leung, K.W., Lim, E.H., Fang, X.S.: 'Dielectric resonator antennas: from the basic to the aesthetic', *Proc. IEEE*, 2012, **100**, (7), pp. 2181–2193
- [10] Yi, H., Qu, S.-W., Chan, C.H.: 'Wideband dielectric resonator terahertz reflectarray'. 2015 IEEE Int. Conf. on Computational Electromagnetics, 2015, pp. 273–274
- [11] Headland, D., Niu, T., Carrasco, E., *et al.*: 'Terahertz reflectarrays and nonuniform metasurfaces', *IEEE J. Sel. Top. Quantum Electron.*, 2016, **23**, (4), pp. 1–1
- [12] Yang, Y., Wang, W., Moitra, P., *et al.*: 'Dielectric meta-reflectarray for broadband linear polarization conversion and optical vortex generation', *Nano Lett.*, 2014, **14**, (3), pp. 1394–1399
- [13] Keller, M.G., Shaker, J., Petosa, A., *et al.*: 'A Ka-band dielectric resonator antenna reflectarray'. 30th European Microwave Conf., 2000, no. 1, pp. 1–4
- [14] Wang, K.X., Wong, H.: 'A wideband millimeter-wave circularly polarized antenna with 3-D printed polarizer', *IEEE Trans. Antennas Propag.*, 2017, **65**, (3), pp. 1038–1046
- [15] Vorobyov, A., Farserotu, J.R., Decotignie, J.-D.: '3D printed antennas for Mm-wave sensing applications'. 2017 11th Int. Symp. on Medical Information and Communication Technology (ISMICT), 2017, pp. 23–26
- [16] Zhang, S.: 'Design and fabrication of 3D-printed planar Fresnel zone plate lens', *Electron. Lett.*, 2016, **52**, (10), pp. 833–835
- [17] Zhang, S., Arya, R.K., Pandey, S., *et al.*: '3D-printed planar graded index lenses', *IET Microw. Antennas Propag.*, 2016, **10**, (13), pp. 1411–1419
- [18] Isakov, D.V., Lei, Q., Castles, F., *et al.*: '3D printed anisotropic dielectric composite with meta-material features', *Mater. Des.*, 2016, **93**, pp. 423–430
- [19] Damaskos: 'Model 600 T open resonator'. [Online]. Available at <http://www.damaskosinc.com/cavity.htm>, accessed 20-June 2017